Available online at www.sciencedirect.com
ScienceDirect
Journal of Photochemistry and Photobiology B: Biology 88 (2007) 163–179
Journal of Photochemistry and Photobiology B:Biology
www.elsevier.com/locate/jphotobiol

Responses of epidermal phenolic compounds to light acclimation: In vivo qualitative and quantitative assessment using chlorophyll fluorescence excitation spectra in leaves of three woody species

L.P.R. Bidel [a,b,*], S. Meyer [c,d], Y. Goulas [e], Y. Cadot [f], Z.G. Cerovic [c,d]

[a] INRA, UMR A-462 SAGAH, 42 rue Georges Morel, BP 6057, F-49071 Beaucouzé, France
[b] INRA, UMR-1097 DIA-PC, Rhizogenesis lab, F-34095 Montpellier, France
[c] Univ. Paris-Sud, F-91405 Orsay, France
[d] CNRS, UMR-8079, Laboratoire d'Ecologie Systématique et Evolution, F-91405 Orsay, France
[e] CNRS, UMR-8359, Laboratoire de Météorologie Dynamique, Ecole Polytechnique, F-91128 Palaiseau, France
[f] INRA, UE-1117 Vigne et vins, 42 rue Georges Morel, BP 6057, F-49071 Beaucouzé, France

Received 4 June 2007; accepted 28 June 2007
Available online 18 July 2007

Abstract

Chlorophyll fluorescence (ChlF) excitation spectra were measured to assess the UV-sunscreen compounds accumulated in fully expanded leaves of three woody species belonging to different chemotaxons, (i.e. *Morus nigra* L., *Prunus mahaleb* L. and *Lagerstroemia indica* L.), grown in different light microclimates. The logarithm of the ratio of ChlF excitation spectra (logFER) between two leaves acclimated to different light microclimates was used to assess the difference in epidermal absorbance (EAbs). EAbs increased with increasing solar irradiance intercepted for the three species. This epidermal localisation of UV-absorbers was confirmed by the removal of the epidermis. It was possible to simulate EAbs as a linear combination of major phenolic compounds (Phen) identified in leaf methanol extracts by HPLC-DAD. Under UV-free radiation conditions, shaded leaves of *M. nigra* accumulated chlorogenic acid. Hydroxybenzoic acid (HBA) derivatives and hydroxycinnamic acid (HCA) derivatives greatly increased with increasing PAR irradiance under the low UV-B conditions found in the greenhouse. These traits were also observed for the HCA of the two other species. Flavonoid (FLAV) accumulation started under low UV-A irradiance, and became maximal in the adaxial epidermis of sun-exposed leaves outdoors. A decrease in the amount of HCA was observed concomitantly to the intense accumulation of FLAV for both leaf sides of the three species. Judging from the logFER, under low UV-B conditions, larger amounts of HCA are present in the epidermis in comparison to FLAV for the three species. Upon transition from the greenhouse to full sunlight outdoors, there was a decrease in leaf-soluble HCA that paralleled FLAV accumulation in reaction to increasing solar UV-B radiation in the three species. In *M. nigra*, that contains large amounts of HCA, the logFER analysis showed that this decrease occurred in the adaxial epidermis, whereas the abaxial epidermis, which is protected from direct UV-B radiation, continued to accumulate large amounts of HCA.

Keywords: Biospectroscopy; Chlorophyll fluorescence excitation spectra; Leaf polyphenols; Shading effect; Light acclimation; UV-absorbers

1. Introduction

Numerous horticultural, dicotyledonous species have exuberant vegetative growth under greenhouse conditions. They have thinner but larger leaves. They are mechanically less rigid and are more fragile than plants grown under field

* Corresponding author. Present address: University of Montpellier 2 (UM2), UMR DIA-PC, IRD-INRA-SupAgro-UM2, Rhizogenesis team, Laboratory of Plant Biochemistry and Physiology CC 024, Bât.15, Place Eugène Bataillon, F-34095 Montpellier cedex 05, France. Tel./fax: +33 0 467 143612.
E-mail address: Luc.Bidel@univ-montp2.fr (L.P.R. Bidel).

1011-1344/$ - see front matter © 2007 Elsevier B.V. All rights reserved.
doi:10.1016/j.jphotobiol.2007.06.002

conditions. This enhanced primary plant growth under greenhouse conditions might be due to the lack of UV-B radiation needed for the induction of flavonols in the leaf epidermis [1]. Jansen et al. [2] showed that UV-B-induced flavonols in the leaf epidermis act as competitive inhibitors of efflux carriers of indol-acetic acid. Furthermore, plants growing under greenhouse conditions are known to be more sensitive to biotic and abiotic stress. Here again, the lack of flavonols is involved. The bactericidal and fungicidal properties of these phenolic compounds (Phen), or their oxidised products, contribute to increased leaf resistance against pathogens [3]. The proportion of different phenolic compounds, flavonoids (FLAV), hydroxycinnamic acids (HBA) and tannins, in leaves is known to be under the control of other environmental factors, including pathogen attack [4], and low temperatures [5]. Flavonol accumulation in leaves has also been found to increase significantly in response to nitrogen starvation [6]. It has been seen that nitrogen fertilisation can be employed to manipulate the flavonol content of vegetative tissues in tomato [6]. So, a better understanding of the environmental control of flavonol accumulation will be useful to improve horticultural practice and to reduce phytochemical input for greenhouse production.

FLAV synthesis was found to be proportional to the UV-B dose received, even in cell culture [7]. In addition, numerous experiments confirmed increasing leaf Phen content with increasing intercepted UV-B doses [8–10]. The more exposed adaxial side of bifacial leaves accumulates larger amounts of FLAV than the abaxial side [11]. In a wide variety of dicotyledonous species, quercetin and kaempferol derivatives are known to be mainly glycosylated and located in epidermal vacuoles where they absorb UV light (*Vitis vinifera* cv; [12] *Arabidopsis thaliana* Heyn, *Beta vulgaris* L., *Nicotiana tabacum* L., *Pisum sativum* L., *Phaseolus vulgaris* L., *Spinacia oleracea* L. [13]). In addition to this epidermal UV-screening by FLAV, the relative contribution of hydroxycinnamic acids (HCA) was a matter of recent debate [14]. Caldwell et al. originally considered FLAV to be the only, or the main, screening pigment [15]. Accordingly, Markstädler et al. [16] found that HCA contribute minimally to UV-B screening in leaves of *Vicia faba* L. Yet, HCA accumulation partly replaces FLAV in *Arabidopsis* mutants that are defective in the first step specific to FLAV biosynthesis, when it is exposed to UV-B [17]. Sheahan [14] and Kolb et al. [12] further suggested that FLAV played only a minor role in *Arabidopsis* UV-screening and that HCA derivatives (sinapate esters) are the main contributors to epidermal screening. Burchard et al. [18] highlighted that HCA are the dominant UV-B protective compounds in the early stages of primary rye leaves development (*Secale cereale* L.), followed by FLAV in later stages and in reaction to UV exposure. Depending on the species, HCA are either largely unaffected by light microclimate [18] or increase with irradiance [12]. In *Phillyrea latifolia* L., full-sun exposed leaves accumulate FLAV in the epidermis, subepidermal layers and trichomes, whereas less-exposed leaves accumulate HCA in these tissues [19]. Some HBA, such as gallic acid, decrease whereas FLAV content increases under higher UV-B radiation levels [20]. A light-induced decrease in the HCA/FLAV ratio was observed by other authors [21]. If the epidermal FLAV metabolism is markedly stimulated by light, epidermal HCA esters and mesophyll FLAV are less responsive, and seem to be under endogenous control of leaf development and differentiation [22]. However, some plant species specifically accumulate HCA in high-light irradiance conditions, and some other species in situation of oxidative stress (i.e. chlorogenic acid in *Mahonia repens* (Lindl.) G. Don [23]; echinacoside in *Ligustrum vulgare* L. [21,24]; gallotannins [25]).

Knowledge of the distribution of different Phen in plant tissue could help in an improved assessment of their physiological role. Peeling off the epidermis has often been used for that purpose (e.g. [11]). Still, this technique is not only destructive but also inapplicable to many woody species. More recently, a spectral non-destructive method was introduced, based on the screening of chlorophyll fluorescence (ChlF) that reveals the components present in the epidermis [13]. By comparing whole leaf ChlF excitation spectra, acquired from 230 to 650 nm on two different leaves (or leaf sides), the type and amount of Phen that differ in their epidermis can be obtained [13]. This technique allows us to compare UV-sunscreening efficiency of leaves acclimated to different microclimates and to investigate the changes in the FLAV/HCA ratio.

The aims of the experiments presented here were: (i) to characterise and to quantify *in vivo* the leaf epidermal Phen of three weedy species during acclimation to different light microclimates; (ii) to discriminate between HCA and FLAV induction during light acclimation; (iii) to compare three species from different chemotaxons known to have different constitutive phenolic compounds; (iv) to assess the local response of FLAV and HCA to UV-radiation by comparing the changes on the two sides of the leaf.

2. Method and materials

2.1. Plant material and experimental design

Three deciduous woody species that accumulate different groups of Phen in their leaves were selected from the pioneering work of Bate-Smith [26]. The leaves of *Morus nigra* L. (*Moraceae*) are thought to accumulate mainly HCA, such as chlorogenic acid, but are is poor in flavonols and anthocyanins. The leaves of *Prunus mahaleb* L. (*Rosaceae*, *Prunoideae*) mainly accumulate quercetin and kaempferol derivatives, two flavonols. The leaves of *Lagerstroemia indica* L. 'Red Imperator' (*Lythraceae*) are described to be poor in both FLAV and HCA. The leaves of these three species are simple and their colour uniform.

The plants were grown in Angers, France (lat. 47°30′N, long. 0.35°W, alt. 56 m) in a glass greenhouse in which shading was installed, and outdoors in a plant nursery near

a meteorological station. Commercial seeds of *Morus* and *Prunus* (Vilmorin, La Ménitré, France) were stratified and sown in January in small pots in the greenhouse. Rooted cuttings of a single *Lagerstroemia* plant were grown in a commercial nursery (Desmartis nursery, Bergerac, France). All seedlings were transplanted in February to 2 L-containers with a peat/perlite mixture (50%, v/v) and supplied with drip irrigation. In the greenhouse, plants were installed on tables oriented north-south to reduce inter-plant shading, at the density of 13 plants per m^2. Nutrient solution, 1.00, 1.73, 1.00, 1.18, 0.57, 0.48 mequiv. L^{-1} of K^+, NO_3^-, Ca^{2+}, Mg^{2+}, H_2PO^{4-} and SO_4^{2-}, respectively, adjusted to pH 6.3, was provided by the drip irrigation system and was recycled. The solution was replaced once a week.

Three types of rectangular shade made of Agryl® P17 and P30 films (Sodoca Manufacturing, France) were used to obtain four light microclimates in the greenhouse, with 14% (INT1), 27% (INT2), 41% (INT3), 68% (INT4, without shade) of the daily global irradiance transmitted on a sunny day. Only data from the most contrasted microclimates (i.e. INT1, INT4 and EXT) were reported in this paper. A fifth set of plants was installed outdoors (EXT) in early May and received 100% photosynthetically active radiation (PAR). Three replicates were used for each light microclimate during April and May. Characteristics of the microclimates are given in Table 1. A UV-B-less treatment (INT4-UV-B) was added in the greenhouse: three plants of each species were placed under a large cylinder made of 100 μm-thick Rhodoid® film (Rhône-Poulenc, Lyon, France), compound derived from cellulose di-acetate, to filter out UV-B and reduce UV-A radiation. Plants were tagged with plastic clips on the stem or petiole of the apical leaf when the shading was put into place so that only leaves developed under the new UV-B-less light microclimate would be studied. Three stems of outdoor *M. nigra* were covered by bottles made of 5 mm-thick glass to protect the leaves from UV-B radiation (EXT-UV-B treatment). In this way, a comparison of homologous leaves belonging to the same plant protected from-and exposed to-ambient UV-B was obtained. Analyses of Phen were carried out on three replicates of 10 leaves of the internodes 4–7 for *M. nigra* and *L. indica*, and on internodes 10 to 13 for *P. mahaleb*. These leaves were chosen because they were approximately horizontal.

2.2. Microclimate characterisation

The global solar irradiance level was recorded with pyranometer sensors LI-200SB (Licor inc., Nebraska, USA) connected to a datalogger (21X, Campbell Scientific, Courtaboeuf, France) each minute and averaged over 30 min. Irradiance spectra were recorded with a portable spectrophotometer (Advantes, Lanion, France) for each light microclimate using the down flux in a vertical direction (Fig. 1). A cosine corrector with a quartz diffuser appropriate for a UV domain was mounted on the quartz optic fibre. The spectroradiometer with an optic fibre was calibrated against a standard deuterium-halogen light source (DH2000 FSH, Avantes, Lanion, France). The spectrophotometer integration time was adjusted between 5 ms to 500 ms to the irradiance level in order to have the best possible signal/noise ratio. The UV fraction was estimated by integrating the 280–320 nm and the 320–400 nm bands, for UV-B and UV-A, respectively, and integrating 400– 700 nm for PAR. In a closed, glass greenhouse, UV-B radiation was virtually absent, and UV-A largely filtered out. However, the greenhouse was aerated with roof vents and lateral vents during sunny days through which UV radiation could penetrate. So light microclimates were characterised on hot sunny days at the solar zenith when the vents were open (Fig. 1). Table 1 summarises the highest irradiance conditions experienced by leaves. The incident photosynthetic photon flux density was calculated from spectral irradiance according to McCree [27] and expressed in μmol photons m^{-2} s^{-1} PAR. The action spectrum for growth response in higher plants by Flint and Caldwell [8], which takes into account both UV-B and UV-A contributions, was used to calculate the biologically active UV radiation (UV_{BE}) for each light regime (Table 1). UV-B irradiance under the Rhodoid filter was not sufficiently high for an accurate measurement with our fibre-optic portable spectrophotometer. It was assessed by multiplying the irradiance spectrum, obtained under greenhouse (INT4), by Rhodoid transmittance measured with the HP spectrophotometer at the laboratory. Because

Table 1
Characteristics of the light microclimates (based on spectra from Fig. 1)

Light treatment	UV-B 280–320 nm	UV-A 320–400 nm	UV_{BE} 280–400 nm	PAR 400–700 nm	Red 655–665 nm	Far Red 725–735 nm
	W m^{-2}	W m^{-2}	Effective W m^{-2}	μmol m^{-2} s^{-1}	μmol m^{-2} s^{-1}	μmol m^{-2} s^{-1}
INT1	n.d.	1.45	0.02	222	9	8
INT4-UV-B	0.01	25.92	0.47	1440	53	22
INT4	0.11	29.49	0.56	1452	53	44
EXT-UV-B	n.d.	25.28	0.47	1497	53	46
EXT	0.86	42.48	0.95	1850	69	63

For each microclimate, photosynthetically-active radiations (PAR) were calculated and expressed in μmol photons m^{-2} s^{-1} according to the conversion factor given by McCree [27]. Biologically-effective UV radiation (UV_{BE}) levels were calculated according to the UV-biological spectral weighting function for plant growth response by Flint and Caldwell [8]. Since UV-B irradiance was not high enough for accurate measurement under Rhodoid filter (INT4-UV-B), it was calculated using its tranmittance spectrum. n.d., not detectable.

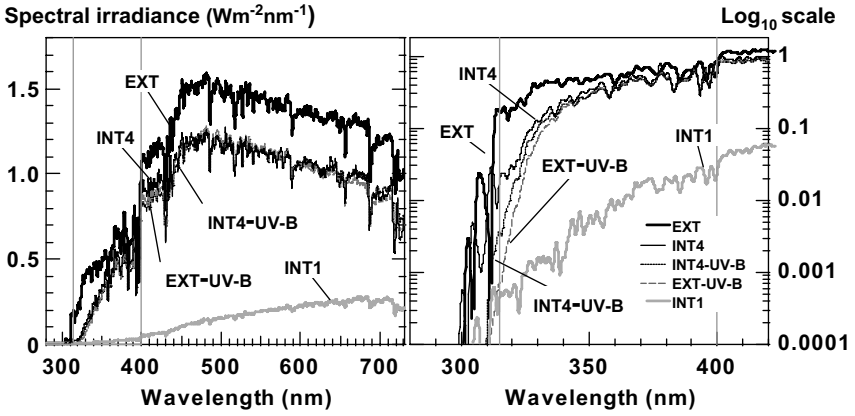

Fig. 1. (a) Irradiance spectra on a horizontal plane of the five light microclimates of this study. They were measured on a clear-sky day in August at Angers (France, lat. 47°30′N, long. 0.35°W, alt. 56 m) at the solar zenith in the normal direction with a cosine corrector. Full sunlight outdoors (EXT), greenhouse without shading (INT4), greenhouse with additional Rhodoid® filter (INT4-UV-B), greenhouse in deep shade (INT1), the interior of a thick glass bottle outdoors (EXT-UV-B). (b) Expressed in log scale. UV-A encompasses the 315–400 nm spectrum as indicated by the vertical lines.

Rhodoid becomes less transparent with ageing when exposed to solar radiation, irradiance filtered through rhodoid under greenhouse conditions decreased by 6 and 3% per month for UV-B and UV-A, respectively. This phenomenon was not taken into account in the present work.

UV-B irradiance intercepted on a horizontal plane was lower than 0.05 W m^{-2} under INT1, INT4-UV-B and EXT-UV-B, and so it was not measurable with the spectrophotometer used. These light treatments can be considered as three nearly UV-free microclimates (Table 1). Instantaneous PAR values recorded at the solar zenith corresponded to 14% and 78% of the PAR intercepted outdoors on a horizontal plane for INT1 and INT4, respectively. Despite the fact that the material used for shading should have behaved as a neutral filter in the visible domain, wavelengths below 650 nm were much more strongly filtered out than above this value. Nevertheless, the proportion of red and far-red radiation of the solar spectrum was preserved (Fig. 1). Consequently, the zeta ratio (Red/Far-red), calculated with values expressed in W m^{-2}, remained equal to 1.11–1.24 among the five microclimates. This corresponds to a theoretical phytochrome photo-equilibrium of 0.69–0.71, calculated according to the formula proposed by Mancinelli [28], which is equal to the theoretical phytochrome photo-equilibrium for full sunlight.

It was not possible to maintain equivalent temperature and hygrometry in the greenhouse and outdoor area during August, the hottest month of the year. The daily average temperature ranged from 14 to 22 °C outdoors, 14–35 °C outdoors within the glass bottle, and 16–26 °C in the glasshouse during the experiment. The lowest temperatures were 9 °C outdoors and 19 °C in the greenhouse. The average temperature difference between the greenhouse and outdoors was less than 5 °C, even on the sunniest day. The difference was 14 °C between outdoors and inside the glass bottle.

2.3. Phenolic compound extraction and HPLC-DAD analysis

For treatments INT1, INT4 and EXT, leaves were collected around the solar zenith at the beginning of June. They were frozen and freeze-dried. Their midribs were removed. Since large quantities of leaf were necessary for this analysis, Phen were determined from 500 mg of fine powder samples of pooled leaves. Each sample was mixed with phloretin as an internal standard, incubated for 24 h in 2 ml of methanol at 4 °C, and then centrifuged at 10,000*g* for 10 min. The supernatant of each sample was filtered through a nylon filter (micro-spin centrifuge filter, mesh = 0.45 μm, Roth, Karlsruhe, Germany). The pellet was extracted twice in 250 μl of methanol by the same procedure. The solvent of the pooled three supernatants was removed using a centrifuge under vacuum at 4 °C and then the extract was dissolved in methanol to a final volume of 1 ml. An aliquot of 20 μl of the extract was injected into an HPLC-DAD. A Waters Alliance HPLC-DA D system (Waters Inc., Milford, USA), provided with a 2695 separation module, a 2996 diode-array detector and the Empower Software, was used. The column was a Merck Lichrospher ODS-2 C18, 5 μm (4.6 × 250 mm) protected by a guard column (10 × 4.6 mm) containing the same material. Solvent (A) was formic acid/water (0.1:0.9, v/v) and solvent (B) was formic acid/water/acetonitrile (0.1:0.6:0.3, v/v/v). The column was equilibrated 5 min before the next injection. The flow rate was 0.8 ml/min. The identification of compounds was based on their retention time and UV-spectra. Phenolic compounds were quantified from the areas of their absorption peaks using multiple-point calibration with external standards at 250 nm for ellagic acid, gallic acid and coniferyl alcohol. Phloridzin, *p*-coumaric acid and vanillin were assessed at 280 nm. Phloretin internal standard, caffeic acid, chlorogenic acid and sinapic acid were assessed at 320 nm. All flavonols were assessed at

360 nm. Quercetin, kaempferol and chlorogenic acid were purchased from Extrasynthèse (Lyon, Nord-Genay, France). Quercetin-3-*O*-glucoside, quercetin-3-*O*-β-D-galactoside, quercitrin, rutin, kaempferol-3-*O*-glucoside, myricetin, apigenin, luteolin, phloretin, phloridzin, coumarin, *p*-coumaric acid, caffeic acid, ferulic acid, sinapic acid, gallic acid and ellagic acid were purchased from Sigma–Aldrich (USA). Each leaf sample was analysed in triplicate. Phenolic compounds were referenced by their retention time.

2.4. Chlorophyll fluorescence excitation spectra

Chlorophyll fluorescence excitation spectra of four fully expanded leaves belonging to the internodes 4–7 for *M. nigra* and *L. indica*, and internodes 10–14 for *P. mahaleb* were recorded on a Cary Eclipse spectrofluorimeter (Varian Inc., Les Ulis, France) equipped with a fibre-optic coupler. Leaves, still attached to the plant in its container, were inserted into a leaf-clip where the optic fibre was tilted to 30° of the leaf surface allowing front-face fluorescence measurement at a constant distance from each leaf.

Chlorophyll fluorescence excitation spectra were scanned from 220 to 650 nm for an emission wavelength of 685 nm, corresponding to the red maximum of chlorophyll emission in intact leaves. It took 20 min to acquire each spectrum. Fluorescence was monitored from a 6 mm-diameter leaf surface at a controlled temperature of 20 °C. Plants were acclimated to 20 °C in the dark for at least 2 h before measurement to insure a dark-adapted state of the photosystem PSII, as recommended by Marksstädtler et al. [16]. Spectra were fully corrected for excitation efficiency and detection response of the spectrofluorimeter and expressed in quinine sulphate-equivalent units (QSEU) as proposed by Cerovic et al. [29]. One QSEU correspond to the fluorescence of 1 pmol ml^{-1} of quinine sulphate in a 1 cm layer of 0.105 mol l^{-1} perchloric acid in water (1 pmol cm^{-2}), excited at 347.5 nm and emitted at 450 nm under identical measuring conditions. The use of this fluorescence standard allows a quantitative comparison among spectra to be obtained from different samples on different days. The logarithm of the ChlF excitation spectra ratio (logFER) provided the absorbance differences between two spectra [13]. The limit of the logFER method is set by the spectrofluorimeter characteristics, its sensitivity, and the proportion of stray light. Excitation spectra recorded on Cary Eclipse were considered reliable when the UV-induced ChlF was above 25 QSEU. This limit corresponds to a transmittance of 3% (or 1.5 absorbance units) computed by comparing UV-induced and green-induced leaf ChlF.

In the present work, all ChlF excitation spectra were normalised prior to logFER calculations, so that the integral between 560 and 590 nm equals one, in order to facilitate quantitative spectral comparisons. For the three plant species, abaxial ChlF excitation spectra were acquired immediately after the adaxial one. This was done only on fully expanded leaves at the same median position on the blade between the major veins. For a given species and leaf side, the logFER between the two different light treatments was calculated with leaves from the same node number. Mean logFER was then calculated using the logFER of the four successive nodes. Whatever the light treatment, no gradient was observed in ChlF along the axis among the fully expanded leaves from the four successive nodes.

Epidermis peeling was not possible for the three species studied. So, in order to obtain naked mesophyll, we removed the upper or lower epidermis by scraping it with a razor blade. Small areas of about 40 mm^2 could be removed, which was sufficient for spectroscopic measurements, but only from thicker leaves grown outdoors (EXT).

2.5. Photosynthetic pigments and leaf mass per area

Chlorophyll *a* and *b*, carotenes and xanthophylls were extracted according to Cartelat et al. [30] from five leaf disks of 5 mm diameter, sampled on the area on which excitation spectra were recorded. The chlorophyll concentration of the extract was calculated using Lichtenthaler's formula [31] and the Chl content was expressed per unit of leaf area. Two other leaf disks of 10 mm diameter were sampled to measure the leaf mass per area (LMA). The leaf disks were dried at 60 °C for 24 h and weighed.

2.6. Statistical analysis and curve fitting

Variance analysis (ANOVA) was used to test the microclimate effect on the phenolic composition of leaves using Statistica (StatSoft Inc., Maison-Alfort, France). Significant differences at $P < 0.05$ between the three microclimates INT1, INT4, EXT were established using Snedecor and Cochran's Student *T*-test [32].

The mean of four ChlF excitation spectra and its standard error (SEM) were calculated for each light treatment using IGOR Pro 4 software (WaveMetrics Inc., Lake Oswego, OR, USA) (cf. Fig. 6). Curves plotted in Figs. 6 and 7 correspond to the best linear combination of the spectra of the phenolic compound standard fitted to match the logFER curves. Spectra of standards dissolved in water at pH 5.5 (average vacuolar pH) were used. Evaluation of the fits was carried out by comparing the root mean squared errors (RMSE) with IGOR Pro-4.

3. Results

3.1. Light effects on leaf properties

The mean LMA of fully expanded leaves decreased 2.9, 5.0 and 5.8 times in the deep shade greenhouse environment (INT1) relative to full sunlight outdoors (EXT) ($P < 0.01$, $n = 20$), for *M. nigra*, *P. mahaleb* and *L. indica*, respectively (Table 2). The Chl was highly variable among fully expanded leaves. However, leaves always had

Table 2
Biomass and contents of photosynthetic pigments for fully-expanded leaves of *M. nigra*, *P. mahaleb* and *L. indica* acclimated to deep shade in the greenhouse (INT1), to non-shaded greenhouse conditions (INT4), and to full sunlight (EXT)

Light microclimates	*Morus nigra* L.			*Prunus mahaleb* L.			*Lagerstroemia indica* L.		
	INT1	INT4	EXT	INT1	INT4	EXT	INT1	INT4	EXT
LMA ($g\ m^{-2}$)	23.3 ± 5.0	35.3 ± 5.2	69.9 ± 10.1	12.2 ± 1.7	37.0 ± 5.1	60.0 ± 9.9	8.5 ± 1.1	23.6 ± 3.5	40.0 ± 9.9
Chl $a+b$($\mu g\ cm^{-2}$)	51.1 ± 10.2	61.6 ± 10.9	38.1 ± 6.9	33.9 ± 4.4	41.6 ± 4.9	30.4 ± 3.1	45.6 ± 15.7	71.5 ± 13.0	47.0 ± 8.0
Chl a/Chl b	2.5 ± 0.0	3.2 ± 0.3	3.6 ± 0.3	2.8 ± 0.2	3.3 ± 0.2	3.3 ± 0.3	2.7 ± 0.1	2.9 ± 0.2	3.3 ± 0.2
$a+b/x+c$	5.7 ± 0.2	4.5 ± 0.1	3.3 ± 0.3	7.6 ± 1.0	6.2 ± 1.2	5.0 ± 0.4	6.3 ± 0.2	6.0 ± 0.6	3.8 ± 0.6

Mean and standard deviation were assessed using 20 and 5 leaves for dried leaf mass per area (LMA) and pigment content expressed on an area basis, respectively. Chl $a+b$ = total chlorophyll content, $x+c$ = total carotenoid content.

significantly higher Chl ($P < 0.05$, $n = 20$) in the greenhouse than outdoors. Even when leaf Chl was not significantly different, or was only weakly different among different light treatments (INT1–INT4), the chlorophyll a/b ratio increased significantly with the PAR ranging from 2.5 to 3.5 ($P < 0.05$, $n = 4$) (e.g. for *M. nigra*). In parallel, xanthophylls largely decreased, so that the Chl/xanthophyll ratio decreased from 3.3 to 5.7 ($P < 0.05$, $n = 4$). These biochemical modifications occurred, and were statistically significant, for the three species. They are known to be a characteristic of acclimation to shade [33].

3.2. Light effects on soluble leaf Phen

The total amount of Phen was the lowest in INT1- and the highest in EXT-treated leaves for the three species ($P < 0.05$, $n = 4$, Table 3). The large increase in Phen in EXT-treated leaves for the three species was mainly due to an increase in quercetin glycoside derivatives. However, under each light condition, the three species differed by their leaf phenolic compositions.

In *M. nigra*, from the INT1 to the EXT microclimate, flavonols and gallic acid derivatives increased considerably. Under INT1, *M. nigra* leaves contained no detectable FLAV and exhibited a very low amount of extractable Phen (Table 3, Fig. 2a). Under INT4 and EXT treatments, leaves accumulated 11 additional compounds with characteristic spectra of flavonols and flavones (Fig. 2a). The four major peaks at 360 nm corresponded to: quercetin-3-*O*-β-D-glucoside (M8, RT = 21.70 min), a quercetin-3-*O*-rutinoside-like compound (M9, RT = 24.35 min), and two kaempferol glycosides (M11 and M12, with RT = 28.35 and 32.30 min, respectively, Fig. 2a and d). They represented 39%, 11%, 22% and 11% of the flavonols, respectively. The amount of myricetin derivatives and compounds with apigenin-like spectra remained quantitatively negligible in the three microclimates compared to quercetin and kaempferol derivatives (less than 3% of FLAV). Free gallic acid derivatives (RT = 11.35 min) increased with irradiance. Their relative proportion was 5%, 16% and 100%, for INT1, INT4 and EXT microclimates, respectively.

The pattern was different for HCA, which increased from INT1 to INT4, but decreased from the INT4 to the EXT microclimate. Under INT1, there were mainly two chlorogenic acid derivatives (M2 peak in Fig. 2a with RT = 5.85 and a much smaller peak at RT = 7.05 min). The number of HCA compounds and the total amount of HCA increased from INT1 to INT4 (Table 3, Fig. 2a). Under INT4 (Table 3) and INT4-UV-B (not shown) microclimates, leaves had significantly more HCA than under INT1 and EXT, and contained the highest amount of caffeic acid and sinapic acid derivatives. In the EXT microclimate, HCA were represented by two chlorogenic acid derivatives (M2 and M3 with RT = 5.10 and 6.90, respectively), two caffeic acid derivatives (RT = 4.50 and 22.65) and a sinapic acid derivative (RT = 37.65) (Fig. 2a). Four minor additional HCA were observed in the INT4 treatment, in particular, a *p*-coumaric acid derivative (RT = 37.30).

For *P. mahaleb* leaves, flavonols, flavones, sinapic acid and coumarin derivatives increased from INT1 to EXT (Table 3). INT1-treated leaves contained flavonol glycoside derivatives, one quercetin type, three kaempferol types and one myricetin type, although these were all very low amounts (Fig. 2b, Table 3). These FLAV can be considered as constitutive. They became minor in INT4- and EXT-treated leaves, which contained six additional quercetin glycoside derivatives. The latter included the two major peaks P4 and P6. Five additional kaempferol glycoside derivatives were present under EXT, including peak P7 (Fig. 2b and e). The total amount of quercetin derivatives increased slightly, but significantly ($P < 0.05$), from INT1 to INT4, and increased drastically from INT4 to the EXT treatment (Table 3). The two predominant flavonols in EXT-treated leaves were two quercetin glycosides (P4 and P6, RT = 14.40 and 21.50 min, respectively, Fig. 2b). They accounted for 61% and 13% of the total amount of flavonols, respectively. Apigenin-like derivatives and phloridzin contents remained low in all microclimates. Among HCA, a large quantity of coumarin derivatives (P3 and P8, at RT = 13.90 and 30.80 min, respectively) increased from INT1 to EXT. Sinapic acid derivative (P9, RT = 40.70 min, Fig. 2b) also increased with irradiance (relative content, 21%, 36%, 100% of HCA, for INT, INT4 and EXT, respectively).

As for *M. nigra*, total HCA in *P. mahaleb* leaves increased from INT1 to INT4 but decreased from INT4

Table 3
Phenolic compounds in methanol extracts of fully expanded leaves of *M. nigra*, *P. mahaleb* and *L. indica* acclimated to deep shade in the greenhouse (INT1), to non-shaded greenhouse conditions (INT4), and to full sunlight (EXT)

Phenolic derivative type	*Morus nigra* L.			*Prunus mahaleb* L.			*Lagerstroemia indica* L.		
	INT1	INT4	EXT	INT1	INT4	EXT	INT1	INT4	EXT
Quercetin glycoside der.	–	21.30 ± 4.60	148.10 ± 34.50	0.02 ± 0.003	0.72 ± 0.06	167.40 ± 46.40	0.87 ± 0.39	7.00 ± 0.61	160.90 ± 32.60
kaempferol glycoside der.	–	3.28 ± 0.40	27.00 ± 5.80	0.10 ± 0.02	0.17 ± 0.03	1.05 ± 0.19	0.07 ± 0.01 ns	0.10 ± 0.01 ns	3.80 ± 0.79
Myricetin glycoside der.	–	6.80 ± 1.30	1.66 ± 0.46	0.39 ± 0.06	–	–	0.07 ± 0.02 ns	0.17 ± 0.02	0.05 ± 0.01 ns
Apigenin-like der.	–	0.55 ± 0.12	1.06 ± 0.24	0.08 ± 0.02 ns	0.12 ± 0.02 ns	0.21 ± 0.04	0.14 ± 0.02	0.31 ± 0.03	18.20 ± 3.69
Phloridzine	–	–	–	0.01 ± 0.01 ns	0.03 ± 0.01 ns	2.72 ± 0.67	0.01 ± 0.00 ns	0.02 ± 0.01 ns	11.50 ± 2.46
Sum of flavonoids	–	31.90 ± 6.50	177.80 ± 40.90	0.60 ± 0.10	1.04 ± 0.12	171.40 ± 47.30	1.16 ± 0.44	7.60 ± 0.70	194.50 ± 39.30
p-Coumaric a. der.	0.11 ± 0.02 ns	0.16 ± 0.04 ns	0.08 ± 0.02 ns	–	–	–	4.81 ± 1.04 ns	0.09 ± 0.01	2.69 ± 0.74 ns
Caffeic a. der.	0.89 ± 0.10	31.80 ± 9.20	5.70 ± 1.85	61.20 ± 11.20	144.60 ± 36.80	0.30 ± 0.10	3.04 ± 0.30 ns	3.49 ± 1.29 ns	0.33 ± 0.10
Chlorogenic a. der.	0.32 ± 0.10	16.10 ± 3.80 ns	17.20 ± 3.02 ns	0.04 ± 0.01	0.01 ± 0.00	–	–	–	–
Sinapic a. der.	–	31.40 ± 9.20	0.15 ± 0.03	5.70 ± 0.50	10.00 ± 1.40	27.40 ± 7.00	0.08 ± 0.01 ns	0.09 ± 0.00 ns	0.24 ± 0.10
Coumarin der.	0.52 ± 0.10 ns	0.83 ± 0.24 ns	0.32 ± 0.10 ns	28.30 ± 2.13	70.60 ± 13.50	156.60 ± 28.20	0.64 ± 0.10	1.45 ± 0.13	4.36 ± 1.00
Sum of HCA	1.83 ± 0.19	80.20 ± 22.50	23.50 ± 5.02	95.20 ± 10.80	225.20 ± 51.70	184.30 ± 35.30	8.60 ± 1.30	5.10 ± 1.30	7.60 ± 1.75
Vanillin-like	–	–	–	31.10 ± 6.10 ns	33.30 ± 5.60 ns	32.30 ± 7.00 ns	0.92 ± 0.17 ns	0.81 ± 0.08 ns	–
Coniferyl alcohol	–	–	–	–	–	–	–	–	104.30 ± 18.50
Gallic and gallic a. der.	2.51 ± 0.36	7.50 ± 2.70	47.90 ± 13.80	0.42 ± 0.03 ns	2.62 ± 0.19 ns	0.63 ± 0.03 ns	33.70 ± 4.80	98.70 ± 10.20	73.70 ± 4.86
Sum of HBA and other der.	2.51 ± 0.36	8.00 ± 2.70	48.00 ± 13.80	32.00 ± 6.20	36.00 ± 5.70	33.00 ± 7.10	35.00 ± 4.80	100.00 ± 10.20	178.00 ± 4.80
Total identified phenolic der.	4.34 ± 0.55	120.00 ± 31.70	249.00 ± 59.72	128.00 ± 17.10	262.00 ± 57.52	388.60 ± 89.70	44.70 ± 6.54	112.70 ± 12.20	380.10 ± 45.85

Mean ± standard deviation of three replicates are expressed in nmol cm^{-2} of leaf for the three treatments. Ellagic acid derivatives are expressed in gallic acid equivalents. ns = not significantly different treatment ($P > 0.05$).

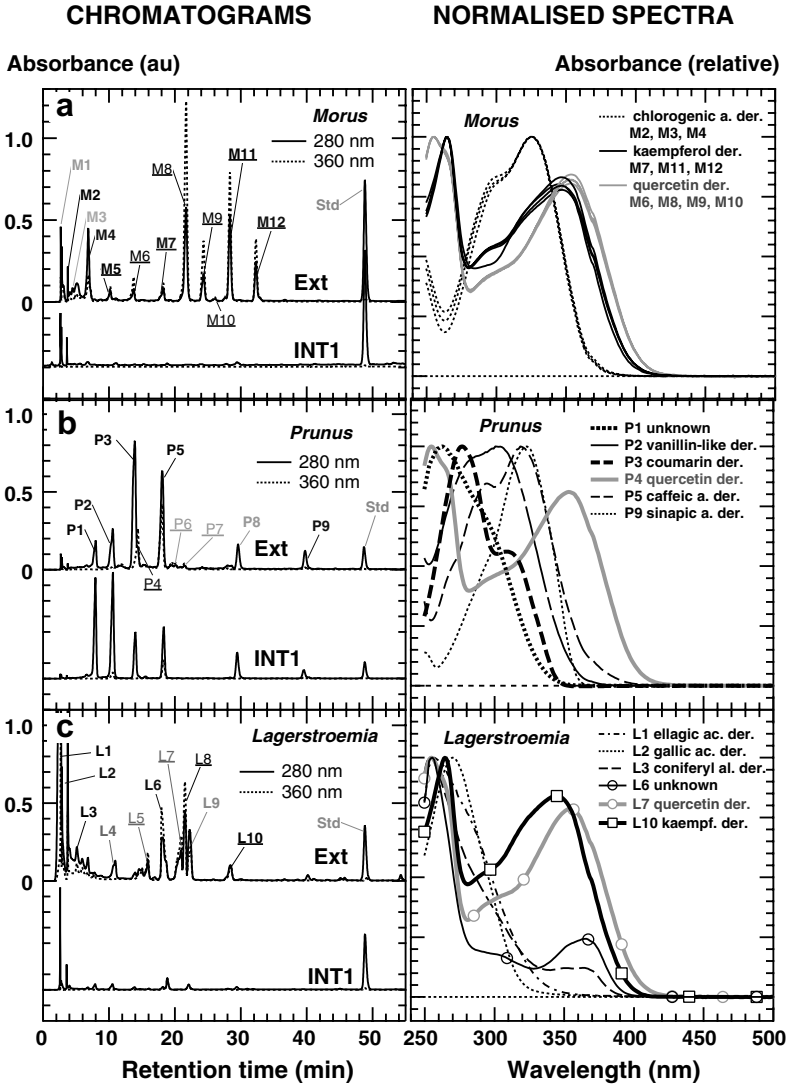

Fig. 2. HPLC-DAD chromatograms of methanol extracts from leaves developed in full sunlight (EXT) and in a greenhouse with heavy shading (INT1) for *M. nigra* (a and d), *P. mahaleb* (b and e) and *L. indica* (c and f). Chromatograms were acquired at 280 and 360 nm. Absorbance values are shown in arbitrary units. Underlined peak numbers refer to FLAV. Absorbance spectra of major chromatographic peaks from full sunlight-grown leaves (EXT) are plotted on the right-hand side (d, e and f). Other peaks: M1, unknown compound; P1, unknown compound at RT = 8.00 min, λ_{max} = 261.5 nm; P6 and P8 quercetin glycoside derivatives; P7, kaempferol glycoside derivative; L1, ellagic acid der. at RT = 2.70 min, λ_{max} = 256.7 nm; L4, p-coumaric acid der.; L5 and L8 quercetin glycoside derivatives; L9, apigenin-like compound. Std, the internal standard, phloretin. The flavonol identity of M8, M9, M11, M12, P4 and P6 peaks was confirmed by acid hydrolysis of the extract. Basic hydrolysis did not modify their retention time and their absorbance spectra.

to EXT (Table 3). This evolution was related to the variation in the amount of caffeic acid derivatives. However, among the eight identified caffeic acid derivatives, the one corresponding to the P5 peak did not follow this trend. Some of the caffeic acid derivatives might be precursors of the sinapic acid derivative (P9, RT = 41.50 min, Fig. 2b). An unidentified compound with a vanillin-like spectrum, (peak P2, RT = 10.60 min) was insensitive to light treatment (Table 3) but largely contributed to the leaf's UV-B absorbance (Fig. 2e). By contrast, the total amount of gallic acid derivatives remained low in all microclimates.

In *L. indica*, total FLAV and ellagic acid derivatives increased from INT1 to EXT, whereas total HCA remained stable between treatments (Table 3). Among FLAV, the major compounds produced under the EXT microclimate were three quercetin glycoside derivatives (L7, L8, and L10 corresponding to RT = 20.90, 21.50 and 28.10 min, respectively, Fig. 2c and f). The relative content of quercetin in INT1-, INT4- and EXT-treated leaves was 0.5%, 4.4% and 100%, respectively. Apigenin-like derivatives also increased from INT1 to EXT microclimates. Among the six apigenin derivatives present, only one was quantitatively important (L9, RT = 23.70 min, Fig. 2c). Like kaempferol glycoside derivatives, there were significant accumulations of phoridzin in leaves, but only under the EXT microclimate. The response of HCA to light microclimates was different from that of FLAV.

INT1-treated leaves already contained coumarin derivatives and these compounds accumulated in INT4 and EXT treatments. The proportions were 15%, 33% and 100%, for the INT1, INT4 and EXT treatment, respectively. However, caffeic acid and *p*-coumaric acid derivatives decreased with irradiance leading to a stable and low total HCA level in all microclimates. So, in contrast to the two previous species, the HCA of *L. indica* remained at low levels and were not always significantly different for the three treatments ($P < 0.05$). HBA, more than HCA, played a major role in UV-B screening in *L. indica*. EXT-treated leaves of *L. indica* produced three coniferyl alcohol derivatives with similar spectra (L3 at RT = 5.10 min, and two other peaks at RT = 5.95, 7.80 min, Fig. 2c and f). A few HBA, with absorbance spectra characteristic of gallic acid derivatives and with varying RT among treatments, were also found (L2, RT = 3.70 min, Fig. 2c and f). These derivatives accumulated more under INT4 than under the EXT microclimate (Table 3). Finally, one compound with an anthocyanin-like spectrum was found at a detectable level with an RT of 10.15 min in INT4 and EXT leaves (not shown). EXT-microclimate leaves contained two additional unknown compounds which contributed largely to UV-B absorbance (Fig. 2c and f). The first one, (L1, RT = 2.70 min), had an absorbance peak at 256.7 nm. The second (L6, RT = 18.30 min) had a first peak at 254.5 nm, a minimum at 328.0 nm and a second peak at 363.6 nm (Fig. 2f).

3.3. Chlorophyll fluorescence excitation spectra of fully expanded leaves

Fig. 3 shows the mean ChlF excitation spectra corresponding to INT1, INT4 and EXT microclimates for the three species. In order to distinguish the relative contribution of UV-absorbers more easily to the form of the spectrum, the measured spectra of Fig. 3a, b and c were equalised in the yellow band and plotted in Fig. 3d, e and f, as described in Method and Materials. For the three species, leaf ChlF excitation by UV-A radiation decreased from INT1 to the EXT microclimate, in agreement with the accumulation of quercetin glycoside derivatives found by

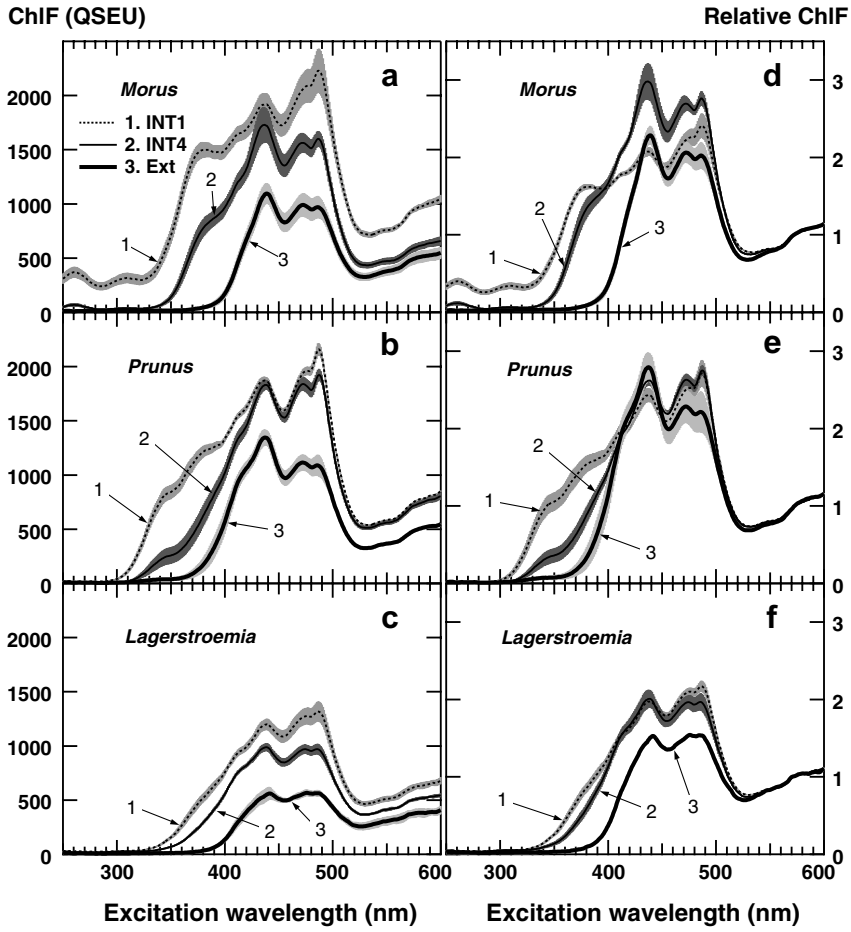

Fig. 3. ChlF excitation spectra of leaves acclimated to deep shade in the greenhouse (INT1 = 1), to the greenhouse without shade (INT4 = 2) and to full sunlight outdoors (EXT = 3), for *M. nigra* (a and d), *P. mahaleb* (b and e) and *L. indica* (c and f). ChlF excitation spectra were monitored on the adaxial surface of the leaf, and expressed in quinine sulphate-equivalent units (QSEU) (a, b and c). For each growth condition, the mean of four spectra and its standard error (SEM) are presented. The emission wavelength was set at 685 nm. In d, e and f, all spectra were normalised so that the integral between 560 and 590 nm equals one, in order to take into account differences in Chl content and tissue scattering among leaves.

HPLC-DAD in each species (cf. Fig. 2). *M. nigra* was the only species in which UV-B radiation could excite ChlF. This was observed only in the INT1-treated leaves (Fig. 3a and d) that contained the lowest amount of Phen (cf. Table 3). The shape of ChlF spectra in the UV-A do main was similar for the three species under the EXT microclimate, but it was different under INT1 and INT4 microclimates. This shows that, under UV-B free microclimates, the ChlF spectra expressed genotypic differences in leaf-soluble Phen compositions. These differences are masked under EXT treatment because of the large accumulation of quercetin glycoside derivatives that largely screens ChlF excitation in all species.

3.4. Epidermal contribution to UV absorbance in outdoors-grown leaves

In the three species, no surface aglycon FLAV were detected by HPLC-DAD in chloroform leaf wash, using the protocol proposed by Vogt et al. [34]. Leaf Phen detected by HPLC-DAD can therefore be present either in the epidermis or in the mesophyll, or in both. We used the logFER method to localise the Phen responsible for UV screening (Fig. 4). We compared intact leaves with naked mesophylls (epidermis scraped away). ChlF excited in the UV increased substantially when the epidermis was removed from the leaf (Figs. 4a, b, and c). Naked mesophyll had a similar ChlF excitation spectrum measured from either the adaxial or abaxial side. This was especially true for normalised spectra of *M. nigra* that continuously overlapped both in the UV and visible parts of the spectrum (Fig. 4a).

The logarithm of the ChlF excitation ratio, logFER, between an intact leaf and its mesophyll corresponds to the absorbance spectrum of compounds present in the epidermis (EAbs). For the three species, logFER was flat and close to zero from 600 nm to around 420 nm, indicating very low epidermal absorbance in the visible part of the spectrum, whereas it increased dramatically below 420–400 nm in accordance with the absorption spectra of Phen.

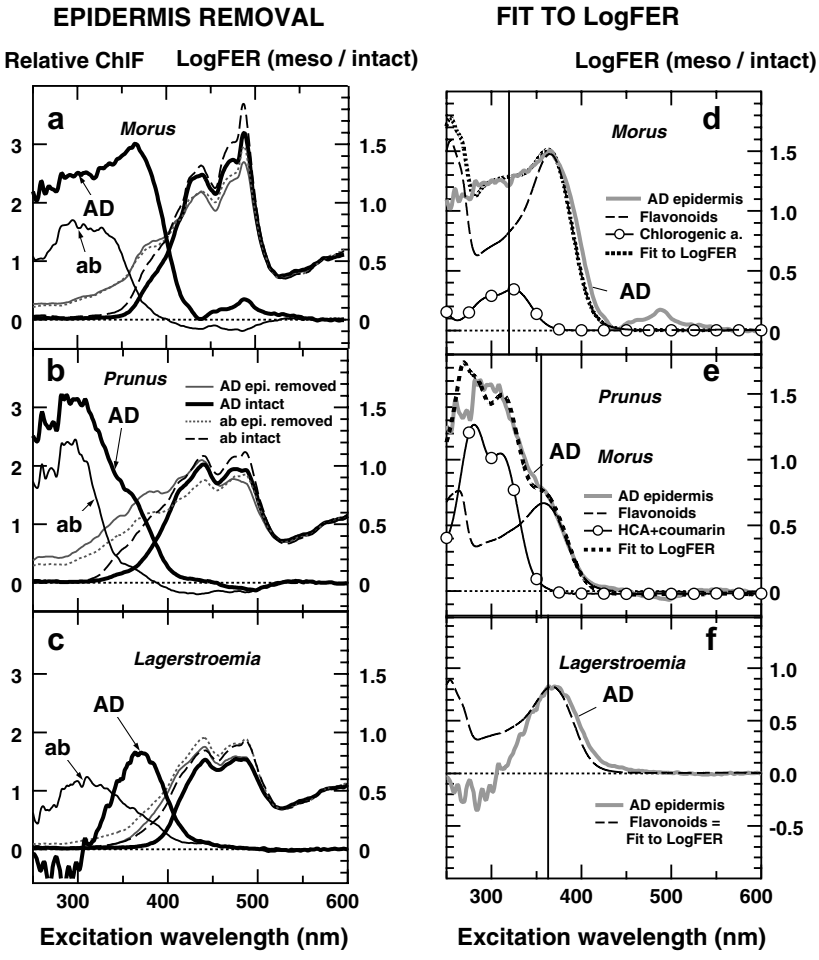

Fig. 4. Comparison of normalised ChlF excitation spectra of intact leaf and mesophyll (after removal of the epidermis) for leaves acclimated to full sunlight (EXT) of *M. nigra* (a), *P. mahaleb* (b) and *L. indica* (c). Solid lines are used for adaxial (AD) leaf sides and dashed lines for abaxial (ab) sides. In graphs a, b and c, logFER are plotted; these are obtained by comparing the naked mesophyll to the intact leaf on the adaxial (AD logFER) and abaxial (ab logFER) sides. Fits to the adaxial logFERs are plotted on the right-hand side graphs (d, e, f) along with combined spectra of standard Phen used for the fit. The vertical line on each graph indicates the detection limit for a reliable logFER calculation.

Therefore, in Figs. 4d, e and f, the measured logFER were compared to the linear combination of absorption spectra of the compounds identified by HPLC-DAD.

For *M. nigra*, a linear combination of the five major compounds present in extracts: quercetin-3-*O*-glucoside (55.2 nmol cm^{-2}); kaempferol-3-*O*-glucoside (16.6 nmol cm^{-2}); rutin (9.9 nmol cm^{-2}); chlorogenic acid (14.4 nmol cm^{-2}); and caffeic acid (13.4 nmol cm^{-2}), permitted us to fit the adaxial EAbs from 280 to 430 nm using concentrations indicated in brackets (Fig. 4d). In this example, flavonols contributed 68%, 82% and 95% to the absorbance at 320, 360 and 375 nm, respectively. The first two wavelengths are usually used to estimate the contribution of HCA and FLAV to EAbs (e.g. [35]), and the third is used for the non-destructive estimation of EAbs in commercial leaf-clips [35]. Chlorogenic acid derivatives contributed 38%, 17% and 5% to EAbs at these three wavelengths, respectively. Overall, this first fit explained 91%, 97% and 100% of the logFER at the three wavelengths considered. Similarly, abaxial logFER could be fitted by the sum of only one flavonol for lower amounts, rutin (17.3 nmol cm^{-2}), a larger amount of chlorogenic acid (28.8 nmol cm^{-2}) and *p*-coumaric acid (19.6 nmol cm^{-2}), and by subtracting small amounts of sinapic acid (−8.4 nmol cm^{-2}) (not shown). The choice of *p*-coumaric and sinapic acid in the last example is only one among several possible HCA combinations to fit EAbs due to the similarity of HCA absorption spectra (cf. Fig. 2).

In *P. mahaleb*, fitting of adaxial EAbs was successful in the 250–450 nm domain (Fig. 4e). The best fit was obtained for a combination of kaempferol-3-*O*-glucoside (24.9 nmol cm^{-2}), rutin (22.3 nmol cm^{-2}), caffeic acid (32.3 nmol cm^{-2}), coumarin (52.1 nmol cm^{-2}) and the unknown compound with a vanillin-like spectrum present in the extract (41.6 nmol cm^{-2}) (cf. Fig. 2e). According to this fit, the sum of flavonols contributed 35%, 95% and 99% to of the absorbance at 320, 360 and 375 nm, respectively. Caffeic acid, coumarin and the vanillin-like compound contributed to a smaller degree to absorbance, and mostly for wavelengths below 310 nm. In contrast to the adaxial side, abaxial EAbs needed a very low amount of flavonols (6.5 nmol cm^{-2} of rutin) combined with caffeic acid (8.1 nmol cm^{-2}), coumarin (63.0 nmol cm^{-2}) and the vanillin-like compound (46.5 nmol cm^{-2}) (not shown).

In *L. indica*, the spectrum of quercetin-3-*O*-glucoside (42.0 nmol cm^{-2}) alone fitted quite well the major logFER peak of the adaxial side of the leaf (Fig. 4f), despite the fact that a large number of compounds were found in the methanol extract. However, the shape of the logFER for wavelengths shorter than 350 nm could not be explained unless the spectrum of compounds absorbing only at shorter wavelength is subtracted. Furthermore, the ChlF excitation spectrum below 320 nm was below the detection limit for several prepared adaxial side mesophylls. Still, the fitted contribution of quercetin derivatives was 99% and 96% of the adaxial EAbs at 360 and 375 nm, respectively.

To sum-up, we showed that logFERs between mesophyll and intact EXT-treated leaves reflect EAbs in the UV-domain, as long as the ChlF amplitude is high enough. LogFER is meaningful for wavelengths longer than 280, 310 and 330 nm for Fig. 4d, e and f, respectively. Fig. 5 shows the close agreement between the EAbs obtained by logFER between the mesophyll and the intact leaf (cf. Fig. 4) and between intact leaves grown under EXT compared to INT1 microclimates. This confirms that the latter non-destructive comparison (logFER) is a good measure of Phen accumulated in the epidermis. Fig. 5 shows that adaxial and abaxial epidermides accumulated HCA in outdoor grown leaves of *M. nigra*.

3.5. Light acclimation of M. nigra leaves

Light acclimation was analysed in the three species by using the INT1-treated leaves as references since they had the lowest UV EAbs.

In *M. nigra*, when INT4-UV-B and INT1 growth conditions were compared, the EAbs difference spectrum of the abaxial leaf side had the shape of a typical HCA absorption spectrum (Fig. 6a). Among the common HCA that were tested, the best fit was obtained with the pure spectrum of chlorogenic acid. Chlorogenic acid was the major HCA found in the extract for this species (Table 3). A large

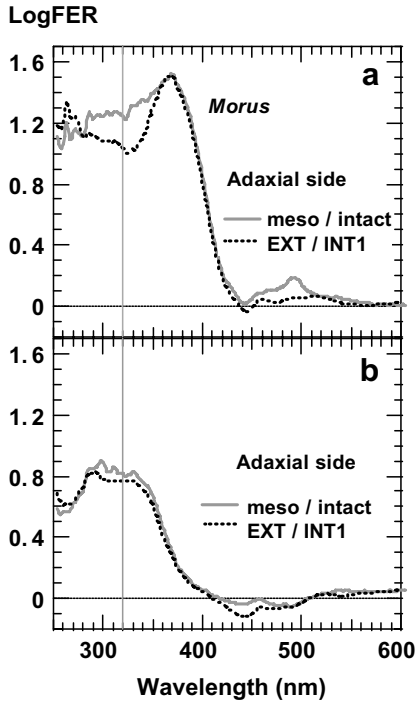

Fig. 5. Comparison of epidermal absorbance obtained by two methods: the logFER obtained by comparing an intact leaf to its mesophyll (after removal of the epidermis) (logFER intact/meso) from Fig. 4a, and the logFER between intact leaves grown in deep shade in the greenhouse (INT1) and in full sunlight outdoors (EXT) (logFER INT1/EXT). Means of four logFER are presented for adaxial (a) and abaxial (b) sides of *M. nigra* leaves. Vertical line: detection limit for reliable logFER.

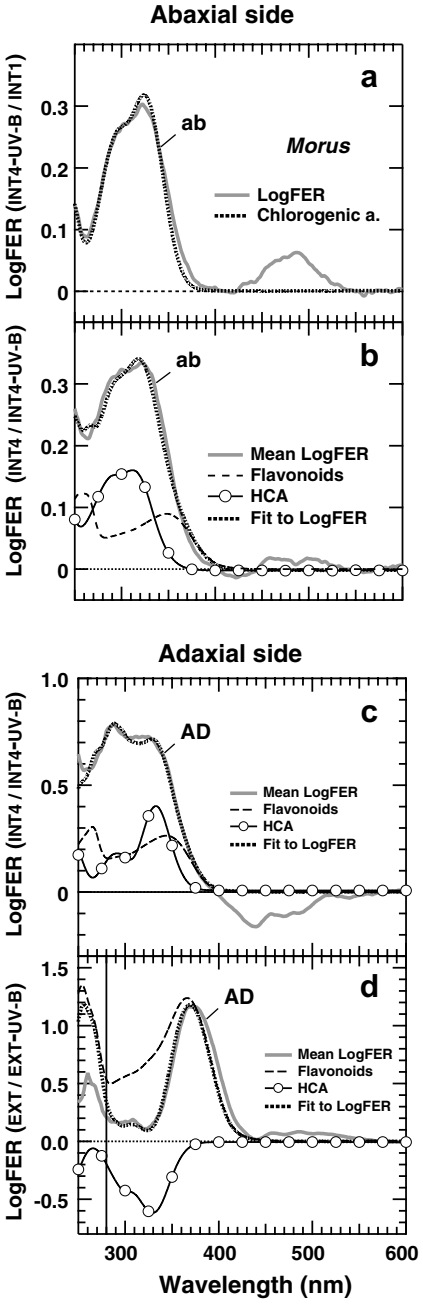

Fig. 6. EAbs differences calculated using logFERs of intact leaves of *M. nigra* among light treatments. Leaves were compared pair-wise among the most shaded leaves (INT1), greenhouse-grown leaves additionally protected from UV-B (INT4-UV-B), greenhouse-grown leaves (INT4), leaves protected from UV-B outdoors (EXT-UV-B), and leaves grown outdoors in full sunlight (EXT). Dotted lines represent the best fits to the logFER obtained as a linear combination of spectra of pure phenolic compounds found in leaf methanol extracts. Means of four logFERs were plotted in b, c and d. A single logFER is plotted in (a) because of a high level of variability. In (d), the vertical line indicates the detection limit for a reliable logFER fit. Abaxial and adaxial side EAbs are shown in a and b, and c and d, respectively.

variability of the amplitude of individual logFERs was observed among leaves from the four successive nodes, but their shape always corresponded to the chlorogenic acid spectrum. Fits revealed that the abaxial epidermis accumulated up to 15.7 nmol cm^{-2} of chlorogenic acid in INT4-UV-B compared to the INT1 treatment.

When INT4 and INT4-UV-B conditions were compared, the shape of the mean logFER spectrum changed in the UV-B domain (Fig. 6b). The fit revealed that the abaxial epidermis accumulated additional amounts of three HCA: chlorogenic acid (6.0 nmol cm^{-2}), caffeic acid (8.1 nmol cm^{-2}), and sinapic acid (3.9 nmol cm^{-2}). They corresponded to the three major HCA found in methanol extracts for INT4-grown leaves (cf. Table 3). The accumulation of a small amount of flavonols (equivalent to 5.0 nmol cm^{-2} of rutin) concomitant to a small UV-B exposure in INT4 was the main difference compared to the pure effect of PAR described in Fig. 6a. Below 320 nm, the fit was improved when gallic acid was added (2.6 nmol cm^{-2}). This compound was also found in the extract (Table 3). The predominant accumulation of several HCA associated with a low proportion of flavonols was also found when comparing EXT to INT4 conditions for the abaxial leaf side that is known to be less exposed to UV radiation than the adaxial side (Fig. 7a).

The logFER spectrum between INT4 and INT4-UV-B obtained for the adaxial side of the leaves (Fig. 6c) was roughly similar to that obtained for the abaxial side (Fig. 6b). The amplitude of logFER, i.e. the EAbs difference, was higher for the adaxial than the abaxial side. However, the fits show that both leaf sides from greenhouse-grown leaves accumulated similar phenolic compounds; only the proportions of individual HCA and FLAV changed for the best fit.

The adaxial EAbs differences between the EXT and the EXT-UV-B treatment showed a peak at 363 nm (Fig. 6d). The curve fitting revealed that it corresponded to an additional accumulation of flavonols comprising 57.6 nmol cm^{-2} of quercetin-3-*O*-glucoside, 24.9 nmol cm^{-2} of kaempferol-3-*O*-glucoside and 4.7 nmol cm^{-2} of rutin. The mean logFER plotted in Fig. 6d had a deep valley located between the benzoyl and the hydroxycinnamoyl band of flavonols. According to the best fit, it can be explained by a decrease in chlorogenic acid (−44.5 nmol cm^{-2}) associated to a smaller accumulation of its precursor, caffeic acid (+26.9 nmol cm^{-2}). Similar results were obtained when the logFER was measured and fitted to compare the adaxial side of INT4- and EXT-treated leaves (Fig. 7b). This was in agreement with the decrease by 30% in total HCA and the increase in FLAV by about 7 times in the whole leaf methanol extract (Table 3). Figs. 6d and 7b show that UV-B radiation promoted a simultaneous decrease in HCA and an increase in FLAV in the adaxial epidermis of *M. nigra*.

In Figs. 6 and 7, changes in the visible part of the spectrum can also be seen in the adaxial logFERs (Fig. 4a). They are attributed to changes in leaf carotenoids (cf. [13]). Although interesting *per se*, light absorption by carotenoids and its transfer to chlorophyll is beyond the scope of the present study.

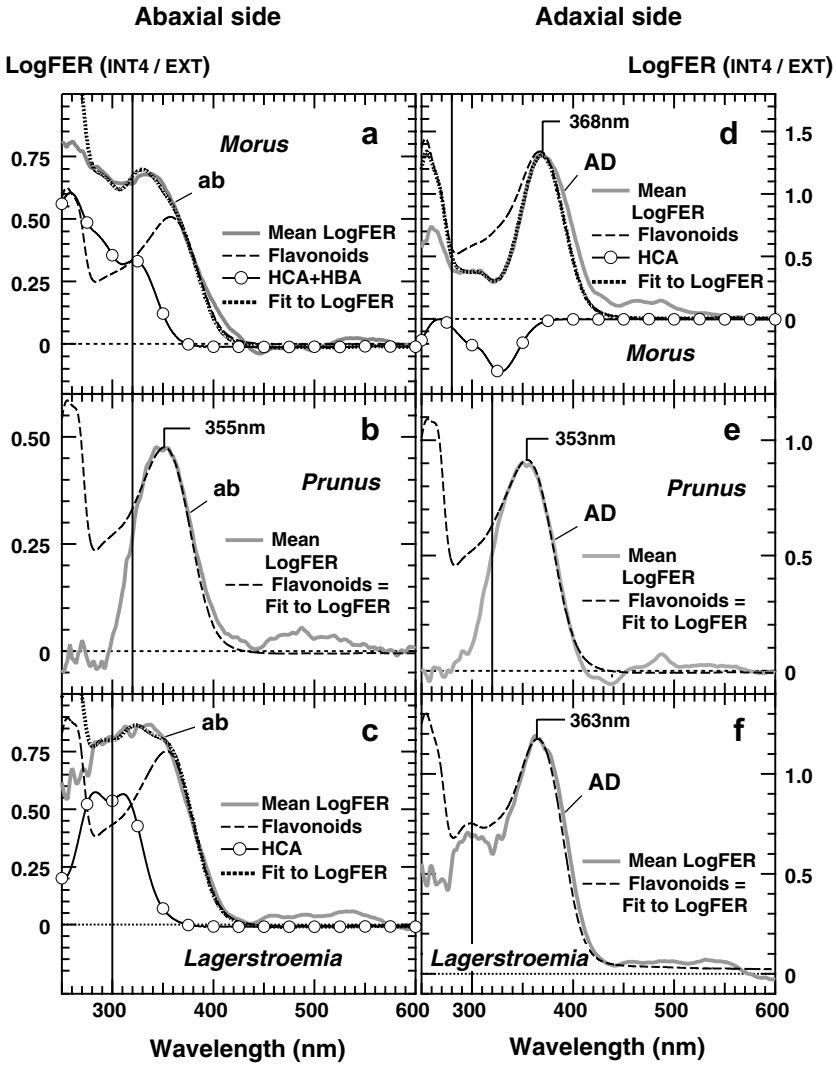

Fig. 7. Epidermal absorbance differences obtained from logFERs between leaves grown in the greenhouse (INT4) and outdoors (EXT) for the abaxial and the adaxial sides of *M. nigra* (a and d), *P. mahaleb* (b and e) and *L. indica* (c and f). EAbs differences were calculated using the mean of four individual logFER derived from normalised ChlF excitation spectra. Dotted lines represent the best fits to the logFER obtained as a linear combination of spectra of pure phenolic compounds found in leaf methanol extracts. In B, E and F, the fit was obtained by a combination of flavonols alone (Fit = FLAV). Vertical line: detection limit for reliable logFER calculation.

3.6. Light acclimation of *P. mahaleb* and *L. indica* leaves

Both *P. mahaleb* and *L. indica* INT1-treated leaves strongly absorbed UV-B by their adaxial side compared to *M. nigra* leaves (cf. Fig. 3). Consequently, the logFER calculation according to Method and Materials could only be reliable in the UV-A radiation and visible spectral domains (Figs. 7c–f). Fig. 7 shows that both leaf sides of *P. mahaleb* and *L. Indica* leaves absorbed more UV-A radiation in the EXT treatment than in the INT4 treatment. This UV-A radiation absorption is fitted mainly by flavonols, and it is higher in adaxial than in abaxial epidermides of EXT-treated leaves (Figs. 7b and c vs. 7e and f). Fig. 7 shows the means of four logFER (as for Fig. 6b–d), that were plotted and fitted, but without SEM. In *P. mahaleb*, the fit of the abaxial logFER revealed that the epidermis accumulated flavonols, equivalent to 14.9 nmol cm^{-2} of rutin and 3.3 nmol cm^{-2} of kaempferol-3-*O*-glucoside (Fig. 7c). The best fit of the adaxial logFER was obtained for an additional amount of pure rutin (59.5 nmol cm^{-2}). The decrease of the total HCA amount found in the methanol extract (Table 3) cannot be observed on the logFER spectra because of the high UV-B absorber content which screens too much the ChlF excitation, whatever the treatment (see Fig. 3 for adaxial ChlF spectra).

In *L. indica*, the fit to the abaxial logFER includes mainly flavonols, equivalent to 44.5 nmol cm^{-2} of two quercetin glycosides, and 1.7 nmol cm^{-2} of kaempferol-3-*O*-glucoside, associated with a small amount of an apigenin-like compound (2.8 nmol cm^{-2}). The latter was also found in the extract (cf. Table 3). Finally, 29.6 nmol cm^{-2} of caffeic acid completed the logFER. EAbs differences for the adaxial side and showed a major peak centred on 363 nm. The best fit was obtained for a mixture of

quercetin-3-*O*-glucoside (63.2 nmol cm^{-2}) and kaempferol-3-*O*-glucoside (14.9 nmol cm^{-2}). The fit using only flavonols was still reliable between 300 and 320 nm.

4. Discussion

The results show a genotypic specificity of soluble phenolic compositions in leaves that contrast with the uniformity of the response to UV-B radiation: all three species produced quercetin glycoside derivatives. This leads us to distinguish constitutive and specific leaf Phen from non-specific and inducible Phen during acclimation to light microclimates, in agreement with Tattini et al. [19]. Results also show that, if conventional HPLC analysis gave the total leaf Phen composition, logFER calculations and curve fitting could reveal the distribution of the major UV absorbers on each side of the leaf. A linear combination of spectra of individual Phen allowed a quantitative estimation of their contribution to abaxial and adaxial epidermal sunscreening under different light microclimates. Most importantly, spectra of Phen dissolved in water at the supposed pH of the vacuole (pH 5.5) could be used for the fitting procedure without needing to invoke spectral shifts, as needed for photosynthetic pigments [36]. Hence, specific and non-specific leaf Phen could be probed by monitoring *in vivo* logFER spectra between two greenhouse microclimates and between greenhouse and outdoor microclimates, respectively. In horizontal leaves, specific and non-specific leaf Phen could also be identified by the comparison of abaxial and adaxial logFER, respectively.

As suggested by Bate-Smith [26] in the chemotaxonomical framework, each species differed by its constitutive protection against high natural irradiance. Leaves of *P. mahaleb* were poor in HBA, but may be constitutively protected in the UV-B domain by caffeic acid derivatives, the vanillin-like compounds, and coumarin, since the logFERs showed that these compounds accumulated in the epidermis. Inversely, *L. indica* leaves remained poor in HCA in all treatments, but may be constitutively protected by high amounts of HBA. Compared to these two species, *M. nigra* leaves lacked constitutive phenolics all together, at least the ones extractible by our methanol protocol. Still, this behaviour might be restricted to well-fertilised seedlings grown under the experimental conditions described here.

Two general trends emerged from the comparison of the three PAR and UV-B protection strategies: firstly, flavonols were accumulated with increasing irradiance in the three species to the same final amount. The most shaded leaves are devoid of flavonols and flavones in *M. nigra*, and low in *P. mahaleb* and *L. indica*. The accumulation response of flavonols to low UV-radiation levels appeared to be more intense in *M. nigra*, a species lacking constitutive UV-B-absorbing phenolic compounds; secondly, in *M. nigra* and *P. mahaleb*, HCA increased with irradiance under greenhouse conditions, characterised by very low UV-B radiation levels, but decreased in full sunlight. The different HCA compounds had their proper dynamics among species and microclimates. Flavonoids may be synthesised at the expense of HCA since they are both derived from the same phenylalanine precursor [37]. In full sunlight, coniferyl alcohol derivatives and phloridzin seem to confer additional UV-B protection in *L. indica*. Similarly, coumarin largely participated in UV-B protection for *P. mahaleb*.

Quercetin was not present in shaded leaves of *M. nigra*, and was only present at residual levels in the two other species, but it was highly inducible under high irradiance for the three species. The logFER method shows that they accumulated in the epidermis, mainly on the adaxial side. This trend has been commonly observed in other species (in *Vitis vinifera* L. [12]; in *Lactuca sativa* L. [38]; in *Fagopyrum tartaricum* Gaertn [39]; in *Brassica napus* L. [40]). Kaempferol derivatives accumulated in significant amounts only in *M. nigra*. They increased much less with irradiance than quercetin derivatives for the three plant species, which is in accordance with the findings of Markam et al. [41]. Measured amounts of flavonols ranged from 4 to 20 mg g^{-1} of leaf dry weight, corresponding to values usually found for well fertilised deciduous woody species grown in full sunlight (*Phillyrea latifolia* L. [19]; *Quercus robur* L. [42]; *Quercus rubra* L. [43]; *Ligustrum vulgare* L. [21]; *Betula pendula* Roth [44]).

Epidermal vacuolar flavonols contribute to protection against UV radiation and high PAR and also against excess production of reactive oxygen species by leaves exposed to high irradiance. They react with hydrogen peroxide during oxidative stress, which occurs in various conditions: freezing or chilling; water or saline stress; severe mineral starvation [6]; aluminium toxicity; high irradiance; and UV-B exposure [45]. Ortho-dihydroxylated flavonols, such as quercetin derivatives that have high antioxidant potential, increased to a greater extent than ortho-monohydroxylated flavonols of the kaempferol type (in *Petunia* × hybrida Vilm. [46]; in *Brassica napus* L. [40]; in *Trifolium repens* L. [47]). Furthermore, the conversion of quercetin derivatives to aglycones is up-regulated by UV-radiation [48]. For example, for tartary buckwheat, *Fagopyrum tataricum* Gaertn, the main epidermal UV-absorber is rutin, a quercetin rutinoside whose accumulation and conversion into free quercetin is UV-B dependent [39]. In addition to flavonols, ortho-dihydroxylated flavones, such as luteolin, increased considerably in comparison to ortho-monohydroxylated flavones, such as apigenin, with lower antioxidant potential (in *Ligustrum vulgare* L. [21]; in *Marchantia polymorpha* L. [49]). Hence, the inducible and non-specific quercetin glycoside accumulation could be considered as a general leaf trait of sun-exposed leaves, in addition to high LMA, high area-based Chl content, and a high photosynthetic capacity.

The present work clearly highlights that epidermis also contain HCA. Initially, the accumulation of HCA was considered to be independent from intercepted light for developing primary leaves in rye [18]. In agreement with results of Kolb et al. [12] for *Vitis vinifera* cv leaves, we found that

methanol-extractable HCA content increased with increasing UV-A and PAR irradiance in the greenhouse for *M. nigra* and *P. mahaleb*. The nature of the HCA accumulated was species-specific. The content of caffeic acid derivatives of the whole limb was particularly enhanced in *P. mahaleb*. Derivatives of sinapic acid, caffeic acid and chlorogenic acid also increased with irradiance under low UV radiation levels in *M. nigra*. In *L. indica*, the HCA remained at very low levels, the UV-B screening function being carried out by gallic acid derivatives that largely increased with irradiance under greenhouse conditions, but decreased under outdoor conditions. Under full sunlight outdoors, coniferyl alcohol derivatives take over. In addition, HCA content cannot be considered as a whole, each individual compound having its own dynamics among the three microclimates and among the species (Table 3). Still, judging from the logFER, under low UV-B radiation (Figs. 6a and b), HCA appeared to be present in the epidermis in higher amounts than flavonols for the three species.

Upon transfer to full sunlight, the HPLC analysis of leaf methanol extracts revealed that there was a decrease in the total amount of HCA that paralleled flavonol accumulation in reaction to increasing solar UV-B radiation in the three species (Table 3). These results are in line with those of Tattini et al. [19], who found a light-induced decrease in HCA/FLAV ratios at the whole-leaf level for *Ligustrum vulgare* L. In *M. nigra*, containing a large amount of HCA, logFER analysis convincingly showed that this decrease occurred in the adaxial epidermis whereas the abaxial epidermis, protected from direct UV-B radiation, continued to accumulate a large amount of HCA (Figs. 6a and b). The abaxial epidermis of the two other species presented similar behaviour. These findings are consistent with observations by Olsson et al. [11] in *Brassica napus* L., where kaempferol glycosides were the most abundant FLAV compounds of the adaxial epidermis, whereas the abaxial epidermis chiefly contained HCA. Likewise, Tattini et al. [19] found that full-sun exposed leaves of *Phyllirea latifolia* L. accumulate FLAV in the adaxial and abaxial epidermides, subepidermal layers and trichomes, whereas less-exposed leaves accumulate HCA in these tissues. In *Ligustrum vulgare* L, Tattini et al. [21] found that palisade parenchyma of sun-exposed leaves mainly accumulated FLAV, whereas it accumulated HCA in the spongy mesophyll. All these results suggest a complete deactivation of the hydroxycinnamate-branch pathways in favour of FLAV biosynthesis when exposed to acute UV-radiation stress [19].

For the three typical outdoor-grown leaves analysed in Fig. 4, at 375 nm, FLAV compounds could explain up to 95%, 99% and 96% of the adaxial epidermal absorbance and up to 83%, 100% and 97% of abaxial absorbance for *M. nigra*, *P. mahaleb* and *L. indica*, respectively. Except for the most shaded leaves, HCA had a reduced contribution to epidermal absorbance at 360 nm, and a negligible contribution at 375 nm. This is in agreement with results obtained in field-grown leaves of *Eucalyptus nitens* Maiden [25] and of *Vicia faba* L. [16]. In the latter case, Markstädler et al. found that HCA accounted for only 5% of the absorbance at 366 nm of methanol extracts from peeled epidermides. Our study confirmed that the measurement of ChlF screening at 375 nm using portable fluorimeters like the Dualex [50] and UV-A PAM [35] is a reliable means to non-destructively assess flavonoid content of the epidermides in the three woody species studied. This can probably be extended to other woody species (cf. [51]).

In conclusion, the accumulation of epidermal UV-absorbers seems to be primarily governed by maximal irradiance and the spectral quality of the intercepted light. Both abaxial and adaxial leaf epidermides seem to conform to the same photocontrol, despite their contrasting anatomical characteristics of typical dicotyledonous species. Epidermis removal experiments showed that the *in vivo* absorbance at 375 nm deduced from ChlF excitation resulted exclusively from flavonols and flavones for the three deciduous species belonging to different chemotaxons. The spectral logFER method [13] was extended by the curve fitting of spectra of individual compounds. This approach applied to light-induced leaf acclimation combined to an HPLC-DAD analysis of the Phen present in the whole leaf, allowed us to localise and identify the different responses of HCA and FLAV to light.

5. Abbreviations

Chl	chlorophyll *a* and *b* content per leaf area
ChlF	chlorophyll fluorescence
EAbs	epidermal absorbance
FarRED	far-red radiation [725–735 nm]
FLAV	flavonoids
HBA	hydroxybenzoic acids
HCA	hydroxycinnamic acids
HPLC-DAD	high-performance liquid chromatography with a diode-array detector
LMA	leaf mass per area
logFER	logarithm of the fluorescence excitation ratio
PAL	phenylalanine ammonia-lyase
PAR	photosynthetically active radiation [400–700 nm]
Phen	phenolic compounds
QSEU	quinine sulphate-equivalent units
RT	retention time
RED	[655–665 nm]
UV	ultraviolet radiation
UV-B	ultraviolet radiation [280–315 nm]
UV-A	ultraviolet radiation [315–400 nm]
UV_{BE}	biologically effective UV radiations

Acknowledgements

The authors thank Pr L.-M. Rivière and Dr. E. Pfündel for their very helpful comments on the manuscript. We also thank Dr. D. Rees, INH, for reviewing the English version of the manuscript. We thank G. Sintes, G. Cyril and J.-N.

Reynaud for their contributions to experimental design in Angers. We thank M. Sigogne, N. Masson and O. Douillet for chlorophyll measurements. The authors also thank C. Guillochereau and R. Champenoit for their contribution to HPLC-DAD analyses. This work was supported by the CNRS program FLUOVEG-GDR 1536.

References

[1] F. Hollósy, Effects of ultraviolet radiation on plant cells, Micron 33 (2002) 179–197.
[2] M.A.K. Jansen, R.E. van den Noort, M.Y.A. Tan, E. Prinsen, L.M. Lagrimini, R.N.F. Thorneley, Phenol-oxidizing peroxidases contribute to the protection of plants from ultraviolet-B radiation stress, Plant Physiol. 126 (2001) 1012–1023.
[3] J. Harborne, C.A. Williams, Advances in flavonoid research since 1992, Phytochemistry 55 (2000) 481–504.
[4] R.A. Dixon, N.L. Paiva, Stress-induced phenylpropanoid metabolism, Plant Cell 7 (1995) 1085–1097.
[5] A. Leyva, J.A. Jarillo, J. Salinas, J.M. Martinez-Zapater, Low temperature induces the accumulation of phenylalanine ammonia-lyase and chalcone synthase mRNAs of Arabidopsis thaliana in a light-dependent manner, Plant Physiol. 24 (1995) 39–46.
[6] A.J. Stewart, W. Chapman, G.I. Jenkins, I. Graham, T. Martin, A. Crozier, The effect of nitrogen and phosphorus deficiency on flavonol accumulation in plant tissues, Plant Cell Environ. 24 (2001) 1189–1197.
[7] E. Wellmann, UV dose-dependent induction of enzymes related to flavonoid biosynthesis in cell suspensions culture of parsley, FEBS Lett. 51 (1975) 105–107.
[8] S.D. Flint, M.M. Caldwell, Field testing of UV biological spectral weighting functions for higher plants, Physiol. Plant. 117 (2003) 145–153.
[9] V.G. Kakani, K.R. Reddy, D. Zhao, K. Sailaja, Field crop responses to ultraviolet-B radiation: a review, Agric. Forest Meteorol. 120 (2003) 191–218.
[10] J. Rozema, L.O. Björn, J.F. Bornman, A. Gaberik, D.P. Häder, T. Trot, M. Germ, M. Klisch, A. Gröniger, R.P. Sinha, M. Lebertd, Y.Y. Hed, R. Buffoni-Hallb, N.V.J. de Bakkera, J. van der Staaija, B.B. Meijkampa, The role of UV-B radiation in aquatic and terrestrial ecosystems-An experimental and functional analysis of the evolution of UV-absorbing compounds, J. Photochem. Photobiol. B 66 (2002) 2–12.
[11] T. Olsson, M. Veti, J.F. Bornman, Epidermal transmittance and phenolic composition in leaves of atrazine-tolerant and atrazine-sensitive cultivars of *Brassica napus* grown under enhanced UV-B radiation, Physiol. Plant 107 (1999) 259–266.
[12] C. Kolb, M.A. Käser, J. Kopecky, G. Zotz, M. Riederer, E.E. Pfündel, Effects of natural intensities of visible and ultraviolet radiation on epidermal ultraviolet screening and photosynthesis in grape leaves, Plant Physiol. 127 (2001) 863–875.
[13] Z.G. Cerovic, A. Ounis, A. Cartelat, G. Latouche, Y. Goulas, S. Meyer, I. Moya, The use of chlorophyll fluorescence excitation spectra for the non-destructive in situ assessment of UV–absorbing compounds in leaves, Plant Cell Environ. 25 (2002) 1663–1676.
[14] J.J. Sheahan, Sinapate esters provide greater UV-B attenuation than flavonoids in *Arabidopsis thaliana* (Brassicaceae), Am. J. Bot. 83 (1996) 679–686.
[15] M.M. Caldwell, R. Robberecht, S.D. Flint, Internal filters: prospects for UV-acclimation in higher plants, Physiol. Plant 58 (1983) 445–450.
[16] C. Markstädler, I. Queck, J. Baumeister, M. Riederer, U. Schreiber, W. Bilger, Epidermal transmittance of leaves of Vicia faba for UV radiation as determined by two different methods, Photosynth. Res. 67 (2001) 17–25.
[17] Y.C. Li, G. Gupta, Photosynthetic changes in soybean with and without nitrogen and Increased carbon dioxide, Plant Sci. 89 (1993) 1–4.
[18] P. Burchard, W. Bilger, G. Weissenböck, Contribution of hydroxycinnamates and flavonoids to epidermal shielding of UV-A and UV-B radiation in developing rye primary leaves as assessed by ultraviolet-induced chlorophyll fluorescence measurements, Plant Cell Environ. 23 (2000) 1373–1380.
[19] M. Tattini, E. Gravano, P. Pinelli, N. Mulinacci, A. Romani, Flavanoids accumulate in leaves and glandular trichomes in *Phullyrea latifolia* exposed to excess solar radiation, New Phytol. 148 (2000) 69–77.
[20] M.C. Rousseaux, R. Julkunen-Tiitto, P.S. Searles, A.L. Scopel, P.J. Aphalo, C.L. Ballaré, Solar UV-B radiation affects leaf quality and insect herbivory in the southern beech tree *Nothofagus antarctica*, Oecologia 138 (2004) 505–512.
[21] M. Tattini, C. Galardi, P. Pinelli, R. Massai, D. Remorini, G. Agati, Differential accumulation of flavonoids and hydroxycinnamates in leaves of *Ligustrum vulgare* under excess light and drought stress, New Phytol. 163 (2004) 547–561.
[22] S. Reuber, J.F. Bornman, G. Weissenbock, Phenylpropanoid compounds in primary leaf tissues of rye (*Secale cereale*). Light response of their metabolism and the possible role in UV-B protection, Physiol. Plant. 97 (1996) 160–168.
[23] S.C. Grace, B.A. Logan, W.W. Adams, Seasonal differences in foliar content of chlorogenic acid, a phenylpropanoid antioxidant, in *Mahonia repens*, Plant Cell Environ. 21 (1998) 513–521.
[24] M. Tattini, L. Guidi, L. Morassi-Bonzi, P. Pinelli, D. Remorini, E. Degl'Innocenti, C. Giordano, R. Massai, G. Agati, On the role of flavonoids in the integrated mechanisms of response of *Ligustrum vulgare* and *Phillyrea latifolia* to high solar radiation, New Phytol. 167 (2005) 457–470.
[25] D.C. Close, C. McArthur, A.E. Hagerman, N.W. Davies, C.L. Beadle, Phenolic acclimation to ultraviolet-A irradiation in *Eucalyptus nitens* seedlings raised across a nutrient environment gradient, Photosynthetica 45 (2007) 36–42.
[26] E.C. Bate-Smith, The phenolic constituents of plants and their taxonomic significance. I. Dicotyledons, J. Linn. Soc. (Bot.) 58 (1962) 95–175.
[27] K.J. McCree, The action spectrum, absorbance and quantum yield of photosynthesis in crop plants, Agric. Meteorol. 9 (1972) 191–216.
[28] A.L. Mancinelli, in: R.E. Kendrick, G.H.M. Kronenberg (Eds.), Photomorphogenesis in Plants, second ed., Kluwer Academic Publishers, Dordrecht, 1994, pp. 211–269.
[29] Z.G. Cerovic, G. Samson, F. Morales, N. Tremblay, I. Moya, Ultraviolet-induced fluorescence for plant monitoring: present state and prospects, Agronomie 19 (1999) 543–578.
[30] A. Cartelat, Z.G. Cerovic, Y. Goulas, S. Meyer, C. Lelarge, J.-L. Prioul, A. Barbottin, M.-H. Jeuffroy, P. Gate, G. Agati, I. Moya, Optically assessed contents of leaf polyphenolics and chlorophyll as indicators of nitrogen deficiency in wheat (*Triticum aestivum* L.), Field Crops Res. 91 (2005) 35–49.
[31] H.K. Lichtenthaler, in: P.K. Stumpf, J.B. Mudd, W.D. Nes (Eds.), The Metabolism, Structure, and Function of Plant Lipids, Plenum Press, New York, 1987, pp. 63–73.
[32] G.W. Snedecor, W.G. Cochran (Eds.), Statistical Methods Applied to Experiments in Agriculture and Biology, Ames, 1972.
[33] B. Demmig-Adams, W.W. Adams, S. Grace, Physiology of light tolerance in plants, Hort. Rev. 18 (1997) 215–246.
[34] T. Vogt, P.G. Gulz, H. Reznik, UV radiation dependent flavonoid accumulation of *Cistus laurifolius* L., Z. Naturforsch. 46c (1991) 37–42.
[35] C.A. Kolb, E.E. Pfündel, Origins of non-linear and dissimilar relationships between epidermal UV absorbance and UV absorbance of extracted phenolics in leaves of grapevine and barley, Plant Cell Environ. 28 (2005) 580–590.
[36] E. Pfündel, E. Baake, A quantitative description of florescence excitation spectra in intact bean leaves greened under intermittent light, Photosynth. Res. 26 (1990) 19–28.

[37] J.W. Blount, K.L. Korth, S.A. Masoud, S. Rasmussen, C. Lamb, R.A. Dixon, Altering expression of cinnamic acid 4-hydroxylase in transgenic plants provides evidence for a feedback loop at the entry point into the phenylpropanoid pathway, Plant Physiol. 122 (2000) 107–116.

[38] A. Romani, P. Pinelli, C. Galardi, N. Mulinacci, M. Tattini, Identification and quantification of galloyl derivatives, flavonoid glycosides and anthocyanins in leaves of *Pistacia lentiscus* L., Phytochem. Anal. 13 (2002) 79–86.

[39] Y. Yao, Z. Xuan, Y. Li, Y. He, H. Korpelainen, C. Li, Effects of ultraviolet-B radiation on crop growth, development, yield and leaf pigment concentration of tartary buckweat (*Fagopyrum tataricum*) under field conditions, Europ. J. Agron. 25 (2006) 215–222.

[40] L.C. Olsson, M. Veit, G. Weissenböck, J.F. Bornman, Differential flavonoid response to enhanced UV-B radiation in *Brassica napus*, Phytochem. 49 (1998) 1021–1028.

[41] K.R. Markham, G.J. Tanner, M. Caasi-Lit, M.I. Whitecross, M. Nayudu, K.A. Mitchell, Possible protective role for 3′,4′-dihydroxyflavones induced by enhanced UV-B in a UV-tolerant rice cultivar, Photosynth. Res. 49 (1998) 1913–1919.

[42] J.-P. Salminen, T. Roslin, M. Karonen, J. Sinkkonen, K. Pihlaja, P. Pulkkinen, Seasonal variation in the content of hydrolyzable tannins, flavonoid glycosides, and proanthocyanidins in oak leaves, J. Chem. Ecol. 30 (2004) 1675–1693.

[43] J.M. Warren, J.H. Bassman, D.S. Mattinson, J.K. Fellman, G.E. Edwards, R. Robberecht, Alteration of foliar flavonoid chemistry induced by enhanced UV-B radiation in field-grown *Pinus ponderosa*, *Quercus rubra* and *Pseudotsuga menziesii*, J. Photochem. Photobiol. B: Biol. 66 (2002) 125–133.

[44] M.L. Laitinen, R. Julkunen-Tiitto, M. Rousi, Foliar phenolic composition of european white birch during bud unfolding and leaf development, Physiol. Plant. 114 (2002) 450–460.

[45] C.A. Mazza, H.E. Boccalandro, C.V. Giordano, D. Battista, A.L. Scopel, C.L. Ballaré, Functional significance and induction by solar radiation of ultraviolet-absorbing sunscreens in field-grown soybean crops, Plant Physiol. 122 (2000) 117–125.

[46] K.G. Ryan, K.R. Markham, S.J. Bloor, J.M. Bradley, K.A. Mitchell, B.R. Jordan, UV-B radiation induced increase in quercetin:kaempferol ratio in normal and transgenic lines of Petunia, Photochem. Photobiol. 68 (1998) 323–330.

[47] R.W. Hofmann, E.E. Swinny, S.J. Bloor, K.R. Markham, K.G. Ryan, B.D. Campbell, B.R. Jordan, D.W. Fountain, Responses of nine *Trifolium repens* L. populations to ultraviolet-B radiation: differential flavonol glycoside accumulation and biomass production, Ann. Bot. 86 (2000) 527–537.

[48] T. Suzuki, Y. Honda, Y. Mukasa, S.J. Kim, Effects of lipase, lipoxygenase, peroxidase, and rutin on quality deteriorations in buckwheat flour, J. Agric. Food. Chem. 53 (2005) 8400–8405.

[49] K.R. Markham, K.G. Ryan, S.J. Bloor, K.A. Mitchell, An increase in the luteolin: apigenin ratio in *Marchantia polymorpha* on UV-B enhancement, Phytochemistry 48 (1998) 791–794.

[50] Y. Goulas, Z.G. Cerovic, A. Cartelat, I. Moya, Dualex: a new instrument for field measurements of epidermal UV-absorbance by chlorophyll fluorescence, Appl. Opt. 43 (2004) 4488–4496.

[51] S. Barthod, Z.G. Cerovic, D. Epron, Can dual chlorophyll fluorescence excitation be used to asses the variation in the content of UV absorbing phenolic compounds in leaves of temperate tree species along an irradiance gradient? J. Exp. Bot. 58 (2007) 1753–1760.